

A STUDY OF THE DUCTILE TEARING MECHANISM DURING SINGLE OVERLOADS

N. Ranganathan, R. Tintillier, B. Bouchet and J. Petit\*

In this study the effect of a single overload on a pregrown fatigue crack was studied in air and vacuum on the aluminum alloy 2024-T351. It is shown here that the K-value at the initiation of static fracture, at a fatigue crack,  $K_d$ , is much lower than the  $K_{IC}$  value.

$K_d$  depends on the thickness and R value, and on the environment. The stretch zone size can be related to the crack tip opening displacement at  $K_d$ . The ductile crack growth after stretch zone formation can be explained in terms of non-linear fracture mechanics parameters. A qualitative explanation is offered to explain the observed effects on the conditions at crack initiation.

### INTRODUCTION

The fracture surfaces of real structures and laboratory fatigue specimens often show dark tongue shaped marks. In the studies of Hudson and Hardrath (1) and Forsyth and Ryder (2) have clearly shown that these "tongues" represent the crack front following a non-uniform crack extension characterized by the crack tunnelling forward on a distance larger in the center of a thick plate than near the edges. The studies of Forsyth (3) and Vlasveld and Schijve (4) have shown that such a phenomenon can occur following the application of a single overload to a pregrown fatigue crack.

Detailed examination of fracture surface shows that the point of application of the overload is characterized by a band, which can be several  $\mu\text{m}$  wide, known as the stretch zone which is followed by dimples in the "tongue" area (2, Von Euv et al. (5)). The existence of dimples is characteristic of a ductile rupture process. These two fractographic features have been found to occur in many metallic materials and in different environments as was shown in references 1,2 Steigerwald and Hanna (6), Bathias and Vancon (7) and Ranganathan and Petit (8).

\* Laboratoire de Mécanique et Physique des Matériaux. UA CNRS 863  
E.N.S.M.A. Rue Guillaume VII - 86034 POITIERS Cedex - France

It has been suggested that in relatively thick plates the stress intensity factor at the beginning of this ductile rupture process can be associated with the plane strain fracture toughness,  $K_{IC}$  (4).

The stretch zone formation has also been studied in detail and is associated with crack tip plastic blunting (Kobayashi et al. (9), Hertzberg (10), Broek (11), Bates and Clark (12) and Brothers et al. (13)). The width of the stretch zone, SZW, is considered to attain a critical value at rupture and has been correlated to different fracture mechanics parameters such as the crack tip opening displacement (11,13), the plastic zone size (13), the J integral value (9), or the effective stress intensity factor range (10).

Another approach to the ductile rupture process has been proposed by Eftis et al. (14) with the introduction of a non-linear toughness parameter  $G_c$  which takes into account the plastic strain energy dissipated during the ductile tearing. Based on this approach, Shanyi Du and Lee (15) and Pouloux and Liebowitz (16) have analysed the evolution of crack length and other parameters during rupture.

In this paper, the results of an ongoing research program on the effect of a single overload on the 2024-T351 aluminum alloy are presented to get a new insight into this ductile tearing process.

Particular attention will be given to the following aspects :

- i) The load at the initiation of rupture and the influence of previous fatigue loading conditions.
- ii) the evolution of the stretch zone width.
- iii) The ductile crack extension (dimpled zone).

The obtained results are analyzed and discussed with respect to existing models.

#### EXPERIMENTAL DETAILS

The tests were conducted on compact tension specimens 75 mm wide in two thicknesses of 10 and 4 mm respectively. The specimen geometry was modified as proposed by Landes and Begley (17), so that the crack opening displacement was measured under the loading axis.

The fatigue crack propagation tests were conducted in air and in vacuum at a frequency of 35 Hz or 20 Hz at two R values of 0.1 and 0.5. One test was also conducted in a  $N_2$  environment containing 3 ppm  $H_2O$ .

The overloads were applied at a frequency of 0.02 Hz, by means of a PDP-11 computer. On each specimen 5 to 6 overloads were applied at different  $\Delta K$  levels varying from 5 to 20  $MPa\sqrt{m}$ .

## FRACTURE CONTROL OF ENGINEERING STRUCTURES – ECF 6

The overload ratio, defined as the ratio of the overload stress intensity factor range ( $\Delta K_{\text{peak}}$ ) to the initial fatigue stress intensity factor range ( $\Delta K_i$ ) was equal to 2.0.

During the tests, three different measurements were made using an X-Y plotter :

- i) The crack opening  $\delta$  with respect to the load P,
- ii) The differential crack opening  $\delta'$  with respect to P,  $\delta'$  being defined as

$$\delta' = \delta - C_0 P \dots \dots \dots (1)$$

where  $C_0$  is the compliance of the specimen with the crack fully open (Kikukawa et al (18)).

- iii) The potential drop V across the crack with respect to P. This measurement was done especially for tests in vacuum.

After the tests, the fracture surfaces were examined optically at low magnifications ( $\times 10$ ) to measure the area of the tongue shaped crack extension. The stretch zone widths were measured in a scanning electron microscope using standard stereographic techniques.

### EXPERIMENTAL RESULTS AND ANALYSIS

#### Stress intensity factor at the onset of crack extension

To detect the onset of crack extension it is necessary to distinguish between the fatigue cycle and the overload cycle.

The evolution of  $\delta$ ,  $\delta'$  and V with respect to P show three distinct phases during a fatigue cycle as can be seen in Fig. 1 which corresponds to a  $\Delta K_i$  of  $15.45 \text{ MPa}\sqrt{\text{m}}$  at an R value of 0.1 in vacuum.

The phase I corresponds to the part of the cycle where the crack is closed due to residual compressive stresses in the plastic wake zone (Elber (19)). The crack opens in the central plane strain region at the load  $P_0$  and the local compliance is now equal to  $C_0$  i.e. that of the specimen with the crack fully open.

In phase II, for  $P > P_0$ , the potential across the crack increases gradually to reach a maximum while there is little change in compliance ( $C = C_0$ ). This increase in potential is attributed to a progressive opening of the plane stress ligaments of the crack near the specimen edges as was shown by Lafarie Frenot and Gasc (20) and Petit and Ranganathan (21).

Near the maximum load there is a decrease in compliance and potential (in vacuum) associated with a secondary closure effect as was shown by Bachmann and Munz (22) and Petit et col. (23).

It should be noted that in phases I and III, the local compliance  $C$  is lower than  $C_0$  in the phase II. Also, according to equation 1, the slope of the  $\delta'$ - $P$  curve is zero in the phase II. In phases I and III the slope of the  $\delta'$ - $P$  curve is positive.

The Fig.2 represents the overload applied just after the cycle described in Fig.1.

It can be seen here that the overload cycle is characterized at first by phase A, where the local compliance becomes equal to  $C_0$ , which can be interpreted as a crack reopening process of the zones closed during phase III. This is confirmed by the evolution of the potential diagram  $V$ - $P$  as the potential reaches  $V_{max}$  in the fatigue cycle. In this phase the  $\delta'$ - $P$  curve become horizontal ( $C = C_0$ ).

For further increase in load, the compliance increases as does the potential while the slope of the  $\delta'$ - $P$  curve becomes negative (corresponding to the increase in compliance).

In this study,  $P_d$ , defined as the load at the end of phase A, is associated with the beginning of crack extension. This definition is similar to that used in Ref. (4), where the authors used similar techniques to detect the onset of crack extension.

For tests in air and in  $N_2$ , only the  $\delta'$ - $P$  curve was analyzed to detect the load  $P_d$ .

The figures 3 and 4 show the evolution of  $K_d$  (corresponding to  $P_d$ ) with respect to  $K_{max}$  of the fatigue cycle in air and vacuum.

The following trends are observed :

i) For the lowest  $K_{max}$  value tested, the load  $P_d$  could not be detected.

ii) For a  $K_{max}$  of  $8 \text{ MPa}\sqrt{\text{m}}$ ,  $K_d$  is about 1.5 times  $K_{max}$ .

iii) The difference between  $K_d$  and  $K_{max}$  decreases as  $K_{max}$  increases.

iv) For a given  $K_{max}$  value,  $K_d$  is higher for 4 mm thick specimens than for 10 mm thick specimens.

v) For tests at  $R = 0.1$ ,  $K_d$  tends towards  $K_{max}$  for a value of  $18 \text{ MPa}\sqrt{\text{m}}$  for 10 mm thick specimens and for a value of  $22 \text{ MPa}\sqrt{\text{m}}$  for thinner specimens

vi) For tests at  $R = 0.5$ ,  $K_d$  coincides with  $K_{max}$  for  $K_{max} > 18 \text{ MPa}\sqrt{\text{m}}$  for 10 mm thick specimens.

The general trend observed in the evolution of  $K_d$  is similar to that reported in Ref.(4) but contrarily to what was observed in Ref.(4),  $K_d$  values in the present study are much lower than the  $K_{IC}$  value for the studied material ( $K_{IC}$  for the 2024-T351 alloy is of the order of  $35 \text{ MPa}\sqrt{\text{m}}$  (24)).

### Stretch zone size

The Fig. 5 shows an example of a stretch zone followed by dimples for a  $\Delta K_i$  of  $15.7 \text{ MPa}\sqrt{\text{m}}$  in air.

Previous studies have attempted to correlate SZW with the peak stress intensity factor due to the overload, Ref.(5), or the J integral value for the overload cycle, Ref.(9). As can be seen here the overload is characterized by the formation of a stretch zone as well as dimples and hence it would seem realistic to separate the stretch zone formation from the subsequent dimple formation.

As the initiation of the ductile tearing corresponds to  $K_d$  defined in this study, SZW is expressed as a function of  $K_d$  in Fig.6.

For the overloads conducted at a  $\Delta K_i$  of  $5.67 \text{ MPa}\sqrt{\text{m}}$ ,  $K_d$  was taken to be equal to the maximum stress intensity factor due to the overload,  $K_{pic}$ . It should be noted in this case that the stretch zone was not uniform all along the specimen thickness and the experimental points correspond to maximum values measured.

The stretch zone is associated with crack tip blunting (10, 12). The CTOD at  $K_d$  is given by

$$\text{CTOD} = 0.5 (K_d^2 / E\sigma_y) \quad (2)$$

where E is the young's modulus :  $72000 \text{ MPa}$  and  $\sigma_y$  the yield strength =  $300 \text{ MPa}$ .

The dotted line in the Fig.6 corresponds to equation 2 and an acceptable correlation is found between SZW and CTOD for  $K = K_d$ .

### Subcritical crack growth

The crack growth after the stretch zone formation is accompanied by a significant amount of plastic deformation.

Firstly the classical J integral value was measured from the  $\delta$ -P curves as suggested in Ref. (17). The average crack growth  $\Delta a$  was measured from fractographic observations as being the ratio of the dimpled area to the thickness.

The Fig.7 shows the evolution of the J integral value with respect to a in 4 mm thick specimens. Also given in this figure is the average curve observed on 10 mm thick specimens as given in Ref.(8).

For high J integral values the static crack growth is higher on 10 mm thick specimens.

The tongue sizes seem to be slightly larger for strong overloads in vacuum as was previously reported in Ref.(8).

Comparison with other toughness parameters

The analysis given in references (14) and (15) suggests the use of non linear fracture mechanics parameters such as  $G_c$  or the plastic energy dissipated to describe crack growth in the non linear range. As proposed in Ref.(14) and by Jones et al. (25), the relationship between the crack opening displacement  $\delta$  and the load P can be represented by a three parameter equation of the type :

$$\delta = C_0 P + k(C_0 P)^n \quad (3)$$

From the definition of  $\delta'$  (equation 1), it can be seen that  $\delta'$  represents the non linear term in equation 3, in the case of pronounced plasticity.

To study of the possible influence of previous fatigue loading on the relationship between  $\delta$  and P, the value of  $\delta'$  for  $P > P_d$  for various overloads is given in figures 8 and 9.

It can be seen from comparing these two figures that the relationship between  $\delta'$  and P stabilizes with a constant slope independent of the previous fatigue loading conditions after a transition phase. This transition phase, however, depends upon the previous fatigue loading. In the case of overloads at low  $\Delta K_i$  values the stabilized phase is not observed at all. At high  $\Delta K_i$  values the stabilized phase is observed immediately after  $P_d$ .

The stabilized phase can be associated with stable crack growth as can be inferred from comparing the slopes of  $\delta'$ -P curves in the case of a rupture test (curve 5-Fig.8).

The average value of n in eqn.3, determined from these curves is 8.47 with a standard deviation of 1.35. The value of 8.47 is approximately equal to the inverse of the static hardening coefficient of the material  $N = 0.11$  (Ranganathan (26)).

Having determined the constants in equation 3, the crack growth after overloads was studied in terms of :

- i) Non linear displacement  $\delta'$  and
- ii) The plastic energy dissipated  $U''_p$

$U''_p$  is evaluated according to the equation given in Ref. (14).

$$U''_p = \frac{nk}{n+1} \left( \frac{1}{C_0} \right)^n P^{n+1} \quad (4)$$

In this relation  $U''$  is evaluated in terms of  $C_0$ , i.e. considering that changes in compliance are small.

Figures 10 and 11 show that linear relationships are observed between  $\delta'$  and  $\Delta a$  and  $U''$  and  $\Delta a$ . Such an evolution has been proposed in Refs.(15) and (16).

### DISCUSSION

The analysis presented here permits the definition of  $K_d$  as being the stress intensity factor at the initiation of ductile tearing.

The stretch zone size can be associated with the CTOD value at  $K_d$  and the subsequent stable crack growth can be described in terms of non linear fracture mechanics parameters such as the J integral value or  $U''_p$ , the plastic strain energy.

The discussion here is focused on the significance of  $K_d$  itself and its evolution, particularly :

- i) Why is  $K_d$  much smaller than the  $K_{IC}$  value ?
- ii) Why should  $K_d$  increase with increasing  $K_{max}$  in the previous fatigue cycle ?
- iii) Could there be a difference in  $K_d$  due to environmental effects : the results presented here indicate that  $K_d$  in vacuum can be higher than in air.

For the first question, it can be argued that  $K_{IC}$  represents the stress intensity factor at fracture and tests for the determination of  $K_{IC}$  are so designed to have a very small plastic zone at the crack tip and in plane strain conditions (27). The test conditions also imply a non significant amount of crack growth of the order of the plastic zone size (for  $K \approx K_{IC}$ ), Knott (28).

$K_d$  as defined in this study, detected by sensitive techniques, can be associated with  $K$  at "first Pop-in" and represents very little crack growth ( $\Delta a \approx 0.01$  mm by the potential technique). In these conditions it is not surprising that  $K_d$  their defined can be much smaller than  $K_{IC}$ . As was shown by Broek (29) the stress intensity factor associated with decohesion at inclusions corresponds to a plastic strain of about 0.4 % in Al-Cu alloys which is much smaller than the critical strain at fracture  $\epsilon_F$  which is associated with  $K_{IC}$ .

For the second question it should be borne in mind that fracture in the specimen thicknesses studied, takes place in a mixed plane stress/plane strain mode and as such no rigorous treatment exists in the literature for such conditions.

A qualitative explanation can be offered based on the observations of Kraft et al. (30) reported in (28). According to these authors the total energy at fracture depends upon the relative proportion of slant to square fracture. Considering  $dW_s/dA$  to be the work done in producing unit area of square fracture and  $dW_p/dv$  to be the plastic work density associated with slant fracture, the following expression is obtained for the total work at fracture (28).

$$dW = \frac{dW_s}{dA} \cdot (1-S) + \frac{dW_p}{dv} \frac{BS^2}{2} \quad (5)$$

The analysis in Refs. (28) and (30) shows that  $dW_p/dv$  is about 10 times as high as  $dW_s/dA$  indicating that the energy at fracture increases proportionally with the increase of slant (shear lip) fracture.

Now, in the present work where overloads were applied at increasing value of  $K_{max}$ , the amount of slant fracture increases as one approaches plane stress conditions as was shown by Vogelsang and Schijve (31). Thus according to the analysis presented above the conditions determining fracture (or fracture initiation) should increase with  $K_{max}$ .

An answer to the third question can also be proposed based on the above analysis.

Any external conditions altering the proportion of slant to square fracture should lead to changes in conditions at fracture initiation.

As was shown in Ref. (31) slant fracture begins at lower  $K$  values in vacuum than in air. This means that for a given  $K$  value the ratio of slant to square fracture can be higher in vacuum thus resulting in an increase in conditions determining fracture initiation.

Similarly differences in  $K_d$  due to a change in thickness or an increase in  $R$  ratio can be qualitatively explained based on differences in the relative amounts of slant to square fracture.

#### CONCLUSIONS

The ductile fracture initiation and subsequent static crack growth at a preformed fatigue crack has been studied on the 2024-T351 aluminum alloy in a large  $\Delta K$  range and two different thicknesses, in air and in vacuum.

The  $K$  value at crack initiation is defined as  $K_d$  and is determined by the compliance variation and by the potential drop technique.



The value of  $K_d$  is much smaller than the static  $K_{IC}$  value.

The stretch zone size is correlated to the crack tip opening at  $K_d$ . The static crack growth after  $K_d$  can be described in terms of non linear fracture mechanics parameters.

The influence of different parameters on  $K_d$  such as initial  $K$  level, environmental effects and the effect of thickness can be qualitatively explained by taking into account the relative amount of slant to square fracture.

#### REFERENCES

- 1 . HUDSON, C.M. and HARDRATH, H.F., "Investigation of the effect of variable-amplitude loadings on fatigue crack propagation patterns : NASA TND-1803, 1963.
- 2 . FORSYTH, P.J.E. and RYDER, D.A., *Metallurgica*, 63, p.117, 1961.
- 3 . FORSYTH, P.J.E. "The causes of Mixed fatigue/tensile crack growth and the significance of microscopic crack behaviour, R.A.E., TR.75143, 1976.
- 4 . VLASVELD, J.A. and SCHIJVE, J., *Fatigue of Engg. Matl. and St.*, 3, p. 129, 1980.
- 5 . Von EUW, E.F.J. et al., ASTM STP 513, Am. Society for testing and Materials, Philadelphia, p.230, 1972.
- 6 . STEIGERWALD, E.A. and HANNA, G.L. "Initiation of slow crack propagation in high strength Materials" Proc. ASTM 62, p. 885 1962.
- 7 . BATHIAS, C and VANCON, M., *Engg. Fract. Mech.* 10, p. 409, 1978.
- 8 . RANGANATHAN, N and PETIT, J, ASTM STP 811, Am. Soc. for testing and Matl., p.464, 1982.
- 9 . KOBAYASHI, H et al. "Recent Research on Mechanical Behaviour of Solids", Univ. of Tokyo Press. p. 341, 1979.
10. HERTZBERG, R.W., *Int. J. of Frac.* 15, p.R69, 1979.
11. BROEK, D. *Engg. Frac. Mech.* 6, p.173, 1974.
12. BATES, R.C. and CLARK, W.G. Jr., *Trans ASM* 62, p.380, 1960.
13. BROTHERS, A.J. et col., ASTM STP 493, Am. Society for testing and Materials, Philadelphia, p.3, 1971.
14. EFTIS, J. et col. *Engg. Frac. Mech.* 7, p.491, 1975.
15. SHANYI DU and LEE, J.D., *Engg. Frac. Mech.* 17, p. 173, 1983.
16. POULOUSE, P.K. and LIEBOWITZ, H., *Engg. Fract. Mech.*, 20, p. 179, 1984.
17. LANDES, J.D. and BEGLEY, J.A., STM STP 560, Am. Society for Testing and Matl. Philadelphia, p.170, 1974.
18. KIKUKAWA, M et col., *J. of. Mat. Sci.* 26, p. 1964, 1977.
19. ELBER, W. ASTM STP 486, Am. Soc. for testing and Mat., Philadelphia, p. 239, 1971.
20. LAFARIE-FRENOT, M.C. and GASC, C. *Fat. of Engg. Matl. and st.* 1, p. 431, 1979.

21. PETIT, J, and RANGANATHAN, N. Proc. Conf. AEFM, Rome, Analytical and Experimental Fracture Mechanics, SIH, GC, Ed. SITJHOFF and NOORDDHOFF pub. p.431, 1980.
22. BACHMANN, V. and MUNZ, D., J. Test. Eval. 4, p. 257, 1976.
23. PETIT, J. et col, Proc. Conf. ECF3, Pergamon Press, UK, p.239, 1980.
24. BUCCI, R.J., Eng. Frac. Mech., 12, p.407, 1979.
25. JONES, D.L., et al., Eng. Frac. Mech., 6, p.639, 1974.
26. RANGANATHAN, N, Doctor of Science Thesis, Univ.of Poitiers, 1985.
27. BROWN, W.F. and SRAWLEY, J.E., ASTM STP 381, Am. Society for Testing and Matls., Philadelphia, p.133, 1965.
28. KNOTT, J.F., Fundamentals of Frac. Mechanics, Ed. Butterworth London, 1973.
29. BROEK, D. Phd Thesis, Univ. of Delft, Netherland, 1971.
30. KRAFFT, J.M. et al. Proc. Symp. Crack propagation, Cranfield, 8, 1961.
31. VOGELSGANG, L.B. and SCHIJVE, J., Fat. of Eng. Matl. and St. 3, p.85, 1980.

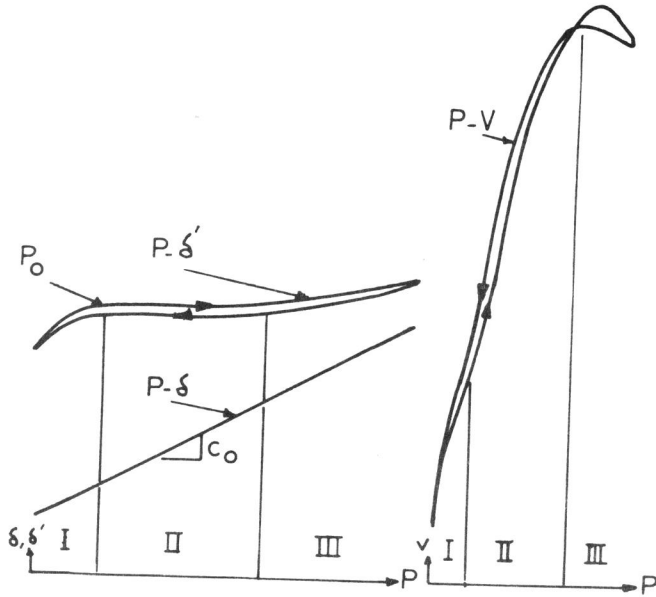


FIG.1 - Examples of  $\delta$ -P,  $\delta'$ -P and V-P diagrams for a fatigue cycle

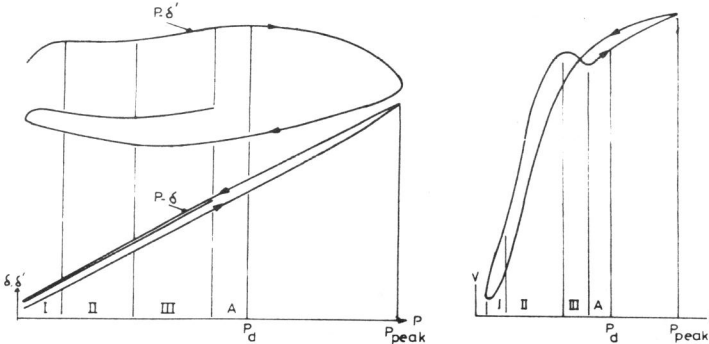


FIG.2 - Same diagrams as in fig.1, for an overload cycle and definition of load  $P_d$ .

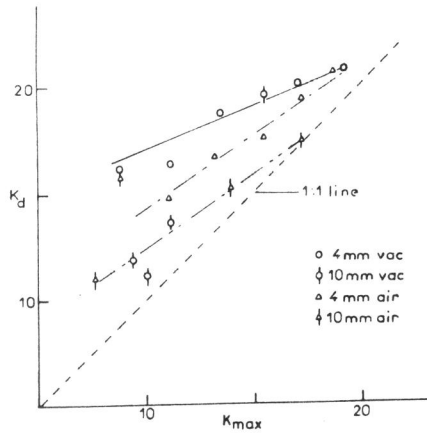


FIG.3-Evolution of  $K_d$  with  $K_{max}$  at  $R = 0.1$

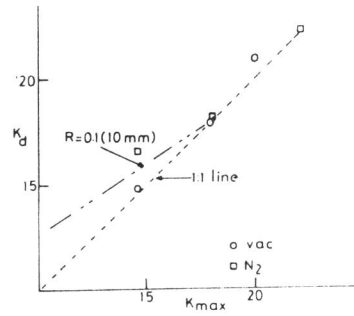


FIG.4- Evolution of  $K_d$  with  $K_{max}$  at  $R = 0.5$

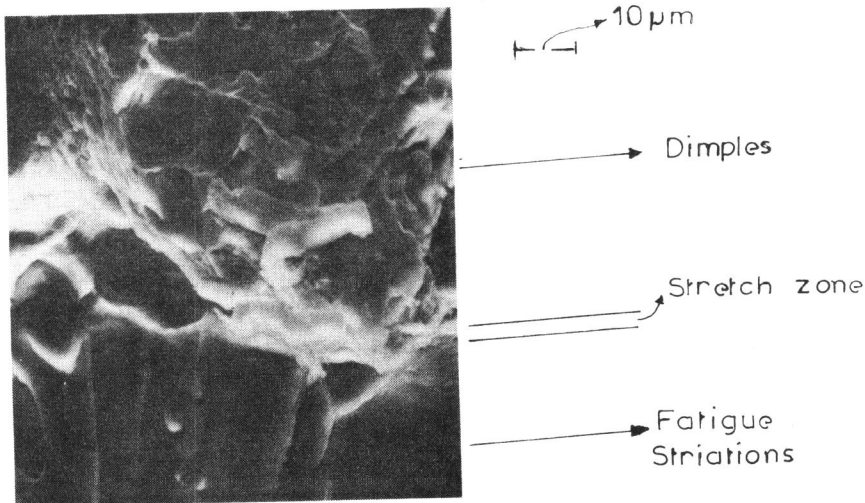


FIG.5- Stretch zone and dimples following an overload.

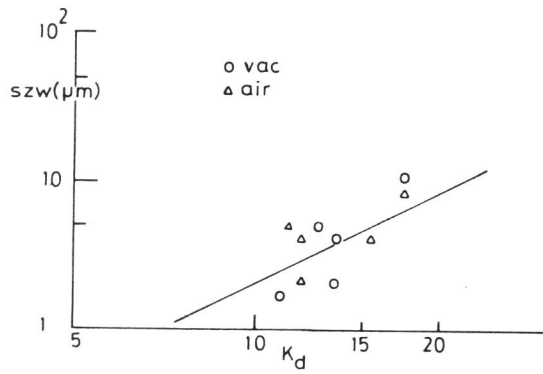


FIG.6- Relationship between S.Z.W and  $K_d$

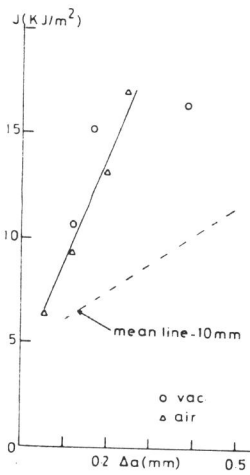


FIG.7- Subcritical crack growth vs. J. integral values.

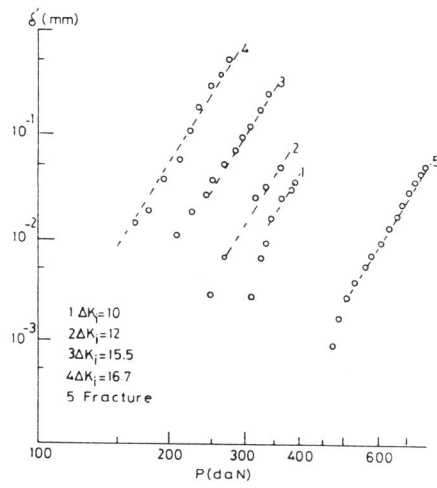


FIG.8- Non linear crack opening  $\delta'$  vs. P, tests in air.

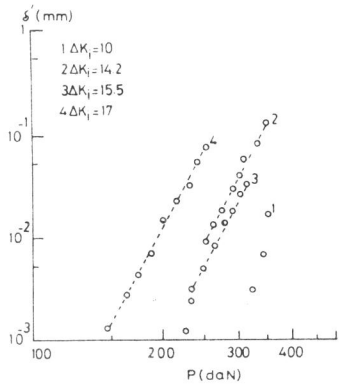


FIG. 9- Same as in fig.8 in vacuum.

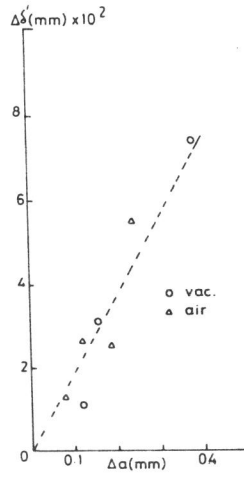


FIG.10- Subcritical crack growth expressed in terms of  $\delta'$ .

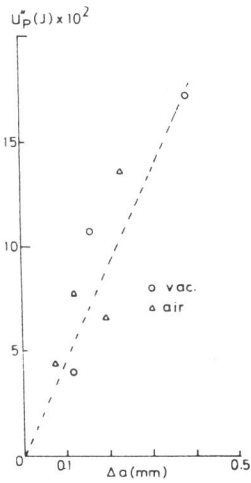


FIG.11- Relationship between plastic strain energy and  $\Delta a$

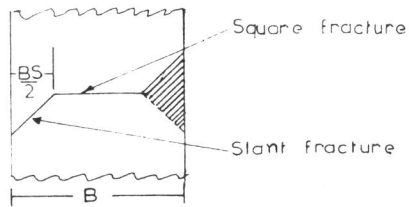


FIG.12- Slant and square fracture in mixed mode conditions.